Learning of Spatiotemporal Patterns in Ising-Spin Neural Networks: Analysis of Storage Capacity by Path Integral Methods

Masahiko Yoshioka

Department of Physics "E.R. Caianiello," University of Salerno, 84081 Baronissi SA, Italy

(Received 5 August 2008; published 13 April 2009)

We encode periodic spatiotemporal patterns in Ising-spin neural networks, using the simple learning rule inspired by the spike-timing-dependent synaptic plasticity. It is then found that periodically oscillating spin neurons successfully reproduce phase differences of the encoded periodic patterns. The storage capacity of this associative memory neural network is enhanced with an adequate level of asymmetry in synapse connections. To understand the properties of these nonequilibrium retrieval states of the neural network, we carry out an analysis based on a path integral method. The relation of a dynamic crosstalk term to time-persistent oscillation of a correlation function well explains the enhancement of the storage capacity in spite of our approximation on nonpersistent terms. We investigate the accuracy of this approximation further by detailed comparison with numerical simulations.

DOI: 10.1103/PhysRevLett.102.158102 PACS numbers: 87.18.Sn, 05.50.+q, 87.10.-e

Measurements of neural activity in a rat's brain have offered a clue to memory representation in the real nervous system [1–3]. These studies have shown that a single neural circuit is capable of storing a number of memories, and the mechanism of this multiple-pattern learning has been explained by multiple attractors in associative memory neural network models [4–16]. It is then an interesting problem to clarify how many memories or attractors can be memorized in one neural network. The upper limit of a number of attractors, namely, storage capacity, has been clarified in the case of the Hopfield model since its symmetric synapse connections allow for the replica calculation based on an energy function [4,5].

The replica method is unavailable with asymmetric synapse connections. Nevertheless, improvement of network performance due to asymmetric connections has also attracted the attention of researchers [6–8]. It is noticeable that asymmetric neural networks are vital for learning about spatiotemporal neural activities. Spatiotemporal learning is also interesting from the biological viewpoint since certain memories in the rat Hippocampus are represented by spatiotemporal neural activities [1,2].

In the present study, we investigate storage capacity of spatiotemporal associative memory in which periodic spatiotemporal patterns are encoded with asymmetric synapse connections due to the learning rule inspired by the spike-timing-dependent synaptic plasticity [12]. During pattern retrieval of this model, spin neurons exhibit periodic oscillation, reproducing phase differences of the encoded periodic patterns. To investigate this nonequilibrium nature of the asymmetric neural network, we analyze the system by path integral methods [8–11,17–21]. Path integral methods can deal with the asymmetric Ising-spin system, such as the asymmetrically modified Sherrington-Kirkpatrick model [10,21]. Using this powerful technique, we evaluate time-persistent oscillation of a correlation function and find the emergence of a dynamic crosstalk term in mean-field equations. Solving these equations, we clarify enhancement of the storage capacity in the region with asymmetric synapse connections.

We define Ising-spin neural network $\sigma_i (i = 1, \ldots, N)$ by the single-spin-flip dynamics with transition rate $w(\sigma_i \to -\sigma_i) = (1/2)[1 - \tanh(\beta \sigma_i h_i)]$, where $h_i = \sum_j J_{ij} \sigma_j$ represents local field and $\beta = 1/T$ represents degree of stochasticity. Periodic spatiotemporal patterns to be encoded are defined by

$$\eta_i^\mu(t) = \cos(t - \phi_i^\mu), \qquad \mu = 1, \ldots, P, \tag{1}$$

where ϕ_i^μ are chosen randomly from the uniform distribution within $[0, 2\pi)$. Our previous study [12] has shown that learning of phases of these periodic patterns is attained by the learning rule of the form

$$J_{ij} = (1/N) \sum_{\mu=1}^{P} \cos(\phi_i^\mu - \phi_j^\mu + \varphi), \qquad i \neq j. \tag{2}$$

This rule gives asymmetric synapses connections $J_{ij} \neq J_{ji}$, except for the case $\varphi = 0$ ($\varphi = \pi$ is meaningless for pattern retrieval). Fixing $J_{ii} = 0$, we make use of Eq. (2) to encode an extensive number of patterns $P = \alpha N$. As shown in Fig. 1(a), asymmetric connections with $\varphi \neq 0$ bring about oscillation of spin neurons, in which the encoded phases are reproduced in the same manner as the previous study [12]. We define overlaps as

$$M^\mu(t) = (1/N) \sum_i e^{i\phi_i^\mu} \sigma_i(t), \qquad \mu = 1, \ldots, P. \tag{3}$$

Owing to the spin oscillation reflecting the encoded phases ϕ_i^1, the overlap for the retrieved pattern shows oscillation $M^1(t) = |M^1| e^{i\omega t}$, where amplitude $|M^1|$ and retrieval frequency ω are constant in time.

To overview storage capacity of the network, we plot results of numerical simulations on the $\varphi - \alpha$ plain in Fig. 2, where high overlap value indicated by white color

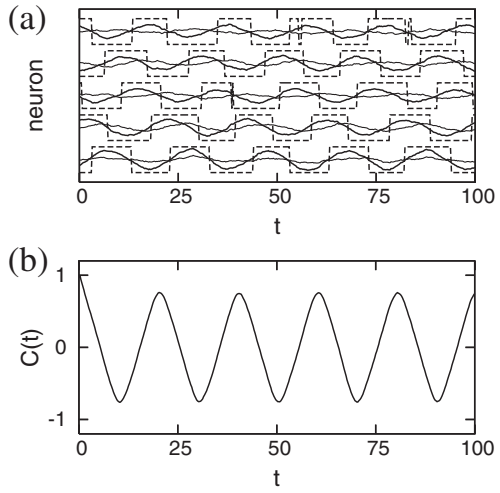

FIG. 1. (a) Periodic oscillations of spin neurons during the retrieval of pattern 1 are plotted for five neurons ($i = 1, \ldots, 5$). The dashed line indicates states of neurons, while the thick and the thin lines represent local field and crosstalk term [i.e., $h_i(t) - \mathrm{Re}(e^{i(\phi_i+\varphi)}M^*(t))$], respectively. The phase differences of the neural oscillations reflect the encoded phases ϕ_i^1. The simulation is carried out under the condition $\varphi = -0.1\pi$, $T = 0.1$, $\alpha = 0.01$, and $N = 10\,000$. The retrieval of pattern 1 is evoked by the initial condition $\sigma_i(0) = H[\eta_i^1(0)]$ with the Heaviside function $H(x)$. (b) The correlation function $C(t)$ obtained from the stationary state in the simulation in (a).

represents success in pattern retrieval. The interesting feature of these phase diagrams is the appearance of the two peaks in the phase boundary with nonzero values of φ. It turns out that asymmetric connections with nonzero φ enhance the storage capacity of the neural networks.

To understand this enhancement of the storage capacity, we begin with analyzing the energy function in the case of symmetric connections $\varphi = 0$, and obtain the replica-symmetric solution $|M| = \langle \int Dz \cos\phi \tanh\beta(|M|\cos\phi + \sqrt{\alpha r}z)\rangle_\phi$, $q = \langle \int Dz \tanh^2\beta(|M|\cos\phi + \sqrt{\alpha r}z)\rangle_\phi$, and $r = q/[2(1 - \beta/2 + \beta q/2)^2]$, where $\langle \ldots \rangle_\phi$ represents the average on ϕ. Then, to find the generalized solution for $\varphi \neq 0$, we analyze the master equation of the system by path integral methods [8–11,17–21], and obtain a single-body dynamics with an effective local field

$$h(t) = \mathrm{Re}(e^{i(\phi+\varphi)}M^*(t)) + \sqrt{\alpha}Z(t) + \alpha \int_{-\infty}^{t} S(t,t')\sigma(t')dt', \quad (4)$$

where $M^*(t)$ represents the complex conjugate of the overlap. The correlation of the crosstalk term $R(t,t') = \langle Z(t)Z(t')\rangle$ and the function $S(t,t')$ satisfy the relations

$$R(t,t') = \sum_{l=0}^{\infty}\sum_{m=0}^{\infty} \cos[(l-m)\varphi]\left[\left(\frac{G}{2}\right)^l \frac{C}{2}\left(\frac{G^\dagger}{2}\right)^m\right](t,t'), \quad (5)$$

$$S(t,t') = \sum_{l=1}^{\infty} \cos[(l+1)\varphi]\left(\frac{G}{2}\right)^l (t,t'), \quad (6)$$

where $C(t,t')$ is a correlation function, $G(t,t')$ is a response function, and $G^\dagger(t,t')$ represents $G(t',t)$. Note that a product among order parameters is defined such that $(GC)(t,t') = \int_{-\infty}^{\infty} G(t,t'')C(t'',t')dt''$.

To find the self-consistent solutions on $R(t,t')$, $S(t,t')$, $C(t,t')$, and $G(t,t')$ for the retrieval state $M(t) = |M|e^{i\omega t}$, we follow the previous studies and decompose the functions into persistent terms and nonpersistent terms: $R(t,t') = r(t-t') + \tilde{R}(t-t')$, $S(t,t') = \tilde{S}(t-t')$, $C(t,t') = c(t-t') + \tilde{C}(t-t')$, and $G(t,t') = \tilde{G}(t-t')$, where we assume $r(t) = r(-t)$, $c(t) = c(-t)$, and $\lim_{t\to\pm\infty} \tilde{R}(t)$, $\tilde{S}(t)$, $\tilde{C}(t)$, $\tilde{G}(t) = 0$. This decomposition makes the analysis easy especially when the system is in the equilibrium state with $\varphi = 0$. In this case, $r(t)$ and $c(t)$ are independent of time [i.e., $r(t) = r$ and $c(t) = c$, where c is equivalent to q in the replica-symmetric solution]. Moreover, the contribution from $\tilde{R}(t)$, $\tilde{S}(t)$, and $\tilde{C}(t)$ can be safely neglected through the fluctuation-dissipation theorem (FDT). In fact, substitution of $\tilde{R}(t) = \tilde{S}(t) = \tilde{C}(t) = 0$ successfully recovers the previous-mentioned replica-symmetric solution.

Our present problem with $\varphi \neq 0$ is, however, more complicated than the equilibrium case with $\varphi = 0$. One difficulty comes from the break of the FDT, which prevents legitimate neglect of $\tilde{R}(t)$, $\tilde{S}(t)$, and $\tilde{C}(t)$. Another difficulty is the periodic oscillation of Ising spins, which gives a periodic persistent term $c(t)$ in the correlation function $C(t)$ as shown in Fig. 1(b). The rigorous treatment of these problems seems difficult. The contribution of the nonpersistent terms are, however, expected to be small at least with small $|\varphi|$. In the following, we thus approximately neglect nonpersistent terms $\tilde{R}(t)$, $\tilde{S}(t)$, and $\tilde{C}(t)$ even with $\varphi \neq 0$, and carry out analysis of the oscillatory persistent term $c(t)$. With this approximation, the local field (4) is

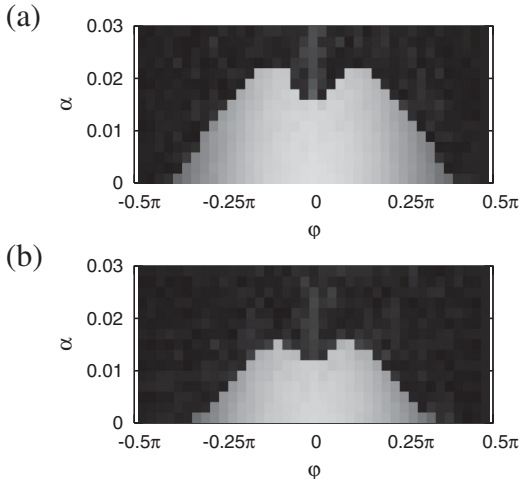

FIG. 2. Absolute values of overlaps $|M|$ in numerical simulations are plotted on the $\varphi - \alpha$ plain both for (a) $T = 0.1$ and (b) $T = 0.2$. White (black) color indicates high (low) absolute overlap in stationary state. For each grid, we conduct one numerical simulation, using $N = 10000$.

rewritten in the form

$$h(t) = |M|\cos(\phi + \varphi - \omega t) + \sqrt{\alpha}z(t), \tag{7}$$

where the correlation of the crosstalk term is given by $\langle z(t)z(t')\rangle = r(t-t')$. The function $r(t)$, which is an even periodic function as $c(t)$, is rewritten as

$$r(t) = \sum_{l=0}^{\infty} r_l \cos(l\omega t). \tag{8}$$

We here focus on solutions with $r_l \geq 0 (l = 0, 1, 2, \ldots)$. Then, $z(t)$ is written as

$$z(t) = \sum_{l=0}^{\infty} \sqrt{r_l}[x_l \cos(l\omega t) + y_l \sin(l\omega t)], \tag{9}$$

where independent stochastic variables x_l and y_l obey a normal Gaussian distribution. From Eq. (5), we obtain

$$r_l = \frac{c_l}{2(1+\delta_{0l})}\left[\frac{1}{1+|\tilde{G}_l|^2/4 - |\tilde{G}_l|\cos(\gamma_l + \varphi)} + \frac{1}{1+|\tilde{G}_l|^2/4 - |\tilde{G}_l|\cos(\gamma_l - \varphi)}\right], \tag{10}$$

where $c_l = [1/(2\pi/\omega)]\int_0^{2\pi/\omega} e^{-il\omega t}c(t)dt$, $\tilde{G}_l = \int_{-\infty}^{\infty} e^{-il\omega t}\tilde{G}(t)dt$, and phase γ_l is defined by $\tilde{G}_l = |\tilde{G}_l|e^{i\gamma_l}$. Note that c_l gives $c(t) = \sum_{l=-\infty}^{\infty} c_l e^{il\omega t}$.

The problem is now reduced into a calculation of order parameters $|M|$, r_l, c_l, g_l, and retrieval frequency ω. From the single-body dynamics with Eq. (7), we obtain

$$dM/dt = -M + \langle e^{i\phi}\tanh\beta[|M|\cos(\phi + \varphi - \omega t) + \sqrt{\alpha}z(t)]\rangle_{\phi,z}, \tag{11}$$

where $\langle\ldots\rangle_\phi$ is the average on ϕ and $\langle\ldots\rangle_z$ is the average on $z(t)$ (i.e., Gaussian distributions on x_l and y_l.) Substituting $M = |M|e^{i\omega t}$, we have

$$|M| = \cos\varphi\langle\cos(\phi)\tanh\beta[|M|\cos\phi + \sqrt{\alpha}z(0)]\rangle_{\phi,z} \tag{12}$$

and

$$\omega = -\tan\varphi. \tag{13}$$

It is notable that within the present approximation, the retrieval frequency ω is given by the simple function of φ. $\tilde{G}_l$ and $\tilde{c}_l$ satisfy the similar relations

$$\tilde{G}_l = \frac{1}{1+il\omega}\langle\beta\tanh'\beta[|M|\cos\phi + \sqrt{\alpha}z(0)]\rangle_{\phi,z}, \tag{14}$$

$$c_l = \frac{1}{1+(l\omega)^2}\langle|\langle e^{il\phi}\tanh\beta[|M|\cos\phi + \sqrt{\alpha}z(\phi/\omega)]\rangle_\phi|^2\rangle_z. \tag{15}$$

The self-consistent solution of Eqs. (9), (10), and (12)–(15) determines all the order parameters. One can show that this solution again recovers the replica-symmetric solution in the limit $\varphi \to 0$.

Finding a numerical solution of the above equations requires another approximation. We first restrict the order of the Fourier coefficients up to n [i.e., we only calculate r_l, c_l, and $\tilde{G}_l (l = 0, \ldots, n)$]. Then, we can readily carry out the average $\langle\ldots\rangle_z$ in Eqs. (12) and (14) since they can be safely replaced by the average on a single Gaussian with variance $\sum_{l=0}^{n} r_l$. This replacement is, however, inapplicable to Eq. (15). To avoid the high-dimensional integrals on x_l and y_l $(l = 0, \ldots, n)$ in Eq. (15), we note $\langle x_l x_m\rangle_z = \langle y_l y_m\rangle_z = \delta_{lm}$ and $\langle x_l y_m\rangle_z = 0$ and carry out an approximation by the second order Taylor expansion:

$$c_l \sim \frac{1}{1+(l\omega)^2}[|I_l^0(1)|^2 + \sum_{m=0}^{n}(|I_l^1(\beta\sqrt{\alpha r_m}\cos m\phi)|^2 + \mathrm{Re}[I_l^2(\alpha\beta^2 r_m\cos^2 m\phi)I_l^{0*}(1)] + |I_l^1(\beta\sqrt{\alpha r_m}\sin m\phi)|^2 + \mathrm{Re}[I_l^2(\alpha\beta^2 r_m\sin^2 m\phi)I_l^{0*}(1)])],$$

with $I_l^p(f) = \langle e^{il\phi}\tanh^{(p)}(\beta|M|\cos\phi)(f)\rangle_\phi$, where $\tanh^{(p)}(x)$ represents its pth derivation. Although we also examined the 4th order expansion, its improvement on the precision was small in spite of large computational costs.

Figure 3 shows the phase diagrams obtained from the above analysis. The two peaks of storage capacity appear in the both phase diagrams, consistently with the simulations in Fig. 2. The results show the high agreement especially with $\varphi = 0$, where our solution is equivalent to the replica-symmetric solution. The agreement is perfect also in the low loading limit $\alpha = 0$. Both in the analysis and the simulations, overlaps show discontinuous change at critical points, except for the case of $\alpha = 0$.

In the region with large $|\varphi|$ and large α, we, however, find disagreement between the theory and the numerical

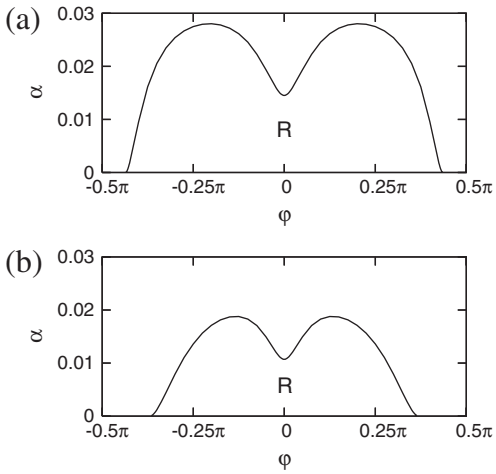

FIG. 3. $\varphi - \alpha$ phase diagrams obtained from the analysis is plotted both for (a) $T = 0.1$ and (b) $T = 0.2$. R represents retrieval phase, in which the analysis yields a retrieval solution with $|M| > 0$. In the analysis, order parameters r_l, c_l, and $\tilde{G}_l$ are calculated up to the 7th order ($n = 7$) with the use of the Taylor expansion on c_l (see text).

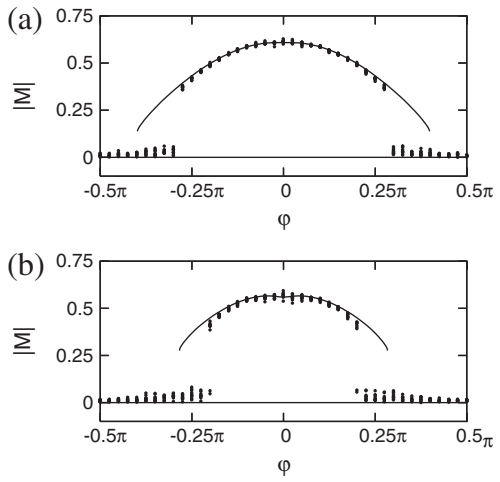

FIG. 4. Overlaps $|M|$ obtained from the analysis with $\alpha = 0.01$ are plotted together with numerical simulations both for (a) $T = 0.1$ and (b) $T = 0.2$. Ten simulations are conducted for each value of φ. Overlaps generally show discontinuous change at critical points, except for the case of $\alpha = 0$.

simulations. In fact, the phase diagrams in Fig. 3 look larger than those in Fig. 2. To illustrate the details of this disagreement, we plot $|M|$ as function of φ in Fig. 4. The deviation between the theory and the simulations increases as $|\varphi|$ increases, and ends up with the phase transition in the simulations before the analytically derived critical points. The size of the overlap in the simulations tends to take a smaller value than that in the analysis, implying the possible presence of additional noisy components in the effective local field. This is considered to be the outcome of nonpersistent terms $\tilde{R}(t)$ and $\tilde{S}(t)$, which are neglected in the present analysis.

We have studied Ising-spin neural networks in which periodic neural activities (1) are memorized with the learning rule (2). During pattern retrieval described in Fig. 1(a), the spin neurons exhibit periodic oscillation with encoded phase shifts ϕ_i^1, yielding overlap oscillation $M^1(t) = |M^1|e^{i\omega t}$. To investigate this dynamic pattern retrieval we have carried out path integral analysis. Both in the analysis (Fig. 3) and in the numerical simulations (Fig. 2), we have found the enhancement of the storage capacity due to asymmetric synapse connections. However, the disagreement between the analysis and the simulations has also been confirmed in the region with the large $|\varphi|$ and the large α, as described in Fig. 4. This has seemed to be the effect of nonpersistent terms in $R(t, t')$ and $S(t, t')$, which are approximately neglected in the present analysis.

Besides the deviation of overlaps, we find deviation of the retrieval frequency ω when $|\varphi|$ is small (data not shown). This indicates the influence of the nonpersistent terms more clearly since Eq. (13) is not suffered from the Taylor expansion on c_l. Further improvement of the analysis requires more general consideration on $R(t, t')$ and $S(t, t')$. One way to ease the problem is the adoption of different network models, as has been demonstrated in a special sort of soft-spin networks [20]. The learning rule resembling Eq. (2) is assumed in oscillator neural networks [14–16]. Attractors of the oscillator networks are, however, effectively fixed-point type, and mean-field equations with a static Gaussian term readily give a good approximation of the storage capacity [16]. These mean-field equations are obtained from signal-to-noise analysis based on an expansion on Thouless-Anderson-Palmer (TAP)-like equation. To carry out signal-to-noise analysis for dynamic attractors as in the present study, one might need to consider an expansion by a response function. [Such expansion indeed gives $R(t, t')$ and $S(t, t')$ for deterministic analog neural networks.] The spatiotemporal learning is not specific to periodic patterns, but available also in nonperiodic patterns [12]. Studying local field oscillation with nonperiodic patterns would also be an interesting problem.

[1] Z. Nádasdy, H. Hirase, A. Czurkó, J. Csicsvari, and G. Buzsáki, J. Neurosci. **19**, 9497 (1999).
[2] D. J. Foster and M. A. Wilson, Nature (London) **440**, 680 (2006).
[3] T. J. Wills, C. Lever, F. Cacucci, N. Burgess, and J. O'Keefe, Science **308**, 873 (2005).
[4] J. J. Hopfield, Proc. Natl. Acad. Sci. U.S.A. **79**, 2554 (1982).
[5] D. J. Amit, H. Gutfreund, and H. Sompolinsky, Phys. Rev. Lett. **55**, 1530 (1985).
[6] G. Parisi, J. Phys. A **19**, L675 (1986).
[7] E. Gardner, H. Gutfreund, and I. Yekutieli, J. Phys. A **22**, 1995 (1989).
[8] A. Düring, A. C. C. Coolen, and D. Sherrington, J. Phys. A **31**, 8607 (1998).
[9] J. Hertz, G. Grinstein, and S. Solla, in *Proceedings of the Heidelberg Colloquium on Glassy Dynamics and Optimization* (Springer-Verlag, Berlin, 1987).
[10] H. Rieger, M. Schreckenberg, and J. Zittartz, Z. Phys. **72**, 523 (1988).
[11] A. C. C. Coolen, arXiv:cond-mat/0006011v1.
[12] M. Yoshioka, S. Scarpetta, and M. Marinaro, Phys. Rev. E **75**, 051917 (2007).
[13] M. Shiino and T. Fukai, J. Phys. A **25**, L375 (1992).
[14] J. Cook, J. Phys. A **22**, 2057 (1989).
[15] A. Arenas and C. J. P. Vicente, Europhys. Lett. **26**, 79 (1994).
[16] M. Yoshioka and M. Shiino, Phys. Rev. E **61**, 4732 (2000).
[17] C. De Dominicis, Phys. Rev. B **18**, 4913 (1978).
[18] H. Sompolinsky and A. Zippelius, Phys. Rev. B **25**, 6860 (1982).
[19] H. Sommers, Phys. Rev. Lett. **58**, 1268 (1987).
[20] A. Crisanti and H. Sompolinsky, Phys. Rev. A **36**, 4922 (1987).
[21] A. Crisanti and H. Sompolinsky, Phys. Rev. A **37**, 4865 (1988).